

Planned science and scientific discovery in equatorial aeronomy

D. L. Hysell ^{1,*}

¹Department of Earth and Atmospheric Sciences, Cornell University, Ithaca, New York, USA

Correspondence*:

D. L. Hysell

david.hysell@cornell.edu

2 *A Perspective article submitted to the Frontiers special issue Generation-to-Generation*
3 **Communications in Space Physics**

4 ABSTRACT

5 This paper discusses the relationship between planning and discovery in science using examples drawn
6 from equatorial aeronomy in general and research at the Jicamarca Radio Observatory in particular. The
7 examples reveal a pattern of discoveries taking place despite rather than because of careful planning.

8 **Keywords:** equatorial aeronomy, incoherent scatter, radar, instability, irregularity, discovery science, serendipity

1 INTRODUCTION

9 Edward Lorenz is famous because of a shortcut he took in 1961. Integrating a small system of
10 differential equations numerically, he initialized the calculations using values from the middle of a
11 prior run to save time. Surprisingly, the solution he found departed rapidly from the prior tabulated
12 result. He traced the discrepancy to minuscule roundoff errors in the values he used for initial
13 conditions. (His computer stored floating point numbers to six decimal places, but he had only
14 printed and then rekeyed them to three.) That small changes in the initial conditions could lead
15 so quickly to drastic changes in the behavior of the system defied common sense. The finding led
16 to chaos theory, raised deep questions about determinism, and doomed prospects for long-range
17 weather forecasting, Lorenz's original problem [42].

18 Undoubtedly, other investigators had encountered similar phenomena in the early days of
19 numerical computing but dismissed them, concentrating instead on the immediate problem at
20 hand. Lorenz is remarkable for having set aside the comparatively routine task before him in favor
21 of getting to the bottom of the "error." His keen judgment, and his freedom to move "off task," led
22 to one of the most important scientific results of the 20th century with impacts beyond Lorenz's
23 discipline.

24 History is full of scientific endeavors which were important because they did not go according to
25 plan. A short list of examples includes Rutherford's discovery of the nucleus, Penzias' and Wilson's
26 discovery of cosmic background radiation, and the Michelson Morley experiment. Space physics and
27 aeronomy is no exception, and it is worth recounting a few more modest but more contemporary
28 examples as reminders of how plans gone wrong remain hallmarks of scientific discovery.

2 EXAMPLES FROM EQUATORIAL AERONOMY AND SPACE PHYSICS

29 Built at about the same time as the Arecibo Observatory, the Jicamarca Radio Observatory was
30 constructed outside Lima, Peru, to demonstrate the possibility of studying the upper atmosphere
31 through the scattering of electromagnetic waves from free electrons [19]. This was to be a cost-
32 effective way of learning about the environment that new spacecraft were being designed to inhabit.
33 For a detailed history of early developments at Jicamarca, see Woodman et al. [57].

34 The motivation for Jicamarca's location was its proximity to the magnetic equator where it would
35 be relatively inexpensive to build a flat antenna to illuminate the ionosphere at an angle normal to
36 the earth's magnetic field. Early intuition about the scattering mechanism held that different ion
37 species, gyrating about the magnetic field lines, would give distinct peaks in the autocorrelation
38 function of the backscattered signal. The ionosphere would in effect become a giant ion mass
39 spectrometer. The required sensitivity of the radar was expected to be substantial, and so a design
40 employing 5 MW transmitter power and an antenna field with a 300 m-squared area was selected.
41 The tests were not expected to take very long.

42 During the build-out of Jicamarca, extensive experiments were performed, and both the theory
43 of scattering from thermal electron fluctuations in a plasma (now known as incoherent scatter)
44 and the experimental techniques required to observe it underwent substantial development. The
45 ion gyroresonances were not observed however. As Farley [13] and Dougherty [11] would show
46 independently, the gyroresonances are largely destroyed by ion Coulomb collisions. Even when the
47 Coulomb collision frequency is much less than the ion gyrofrequency, the gyroresonance cannot
48 be observed if the deviation of the electron position over a gyroperiod is comparable to the radar
49 wavelength divided by 4π . Later, Farley [15] would observe the gyroresonance for H⁺ ions (see also
50 Rodrigues et al. [49]), but the O⁺ gyroresonance cannot be detected given nominal ionospheric
51 conditions.

52 So early experiments at Jicamarca did not go according to plan, but were they a failure? Hardly.
53 To begin with, the experiments provided a basis for much deeper quantitative understanding
54 of incoherent scatter and the practical methods required to make it useful. These include an
55 understanding of the interpretation of the scattering cross section, practical means of measuring
56 absolute electron densities, and theory and methods for inferring ion composition and electron and
57 ion temperatures from the autocorrelation function [5, 4, 14]. Within a few years, the incoherent
58 scatter technique had fulfilled its promises and could be used to measure the most important state
59 parameters of ionospheric plasmas. The techniques were equally applicable at non-equatorial sites.
60 ISR remains the most incisive tool for ground-based remote sensing of the ionosphere.

61 Had construction waited on a more complete knowledge of ISR theory, it is unlikely that an
62 incoherent scatter radar would have been built at the magnetic equator. It is fortunate that it was
63 because this led directly to an enormous range of discoveries in aeronomy that would otherwise
64 have been greatly delayed. Some of these discoveries are at the center of contemporary research in
65 equatorial aeronomy, space physics, and space weather.

66 2.1 The temperature ratio problem

67 By the 1980s, plasma state parameter estimates including electron and ion temperature, ion
68 composition, plasma drift, and electron number density were being measured at ISR facilities
69 around the world and deposited in databases. The procedure involved measuring and fitting the

70 scattered signal autocorrelation function to ISR theory. An inconsistency appeared in the results for
71 Jicamarca, however, were the electron-to-ion temperature ratio at night was found to be consistently
72 less than unity. This is not physically reasonable. There seemed to be a problem, but was it with
73 the experiment or with ISR theory?

74 Other facilities were not reporting difficulties with the temperature ratio, and archival data from
75 early measurements at Jicamarca did not exhibit the problem either, so it was assumed that a
76 bias had crept into the modern experiment. A painstaking analysis of errors and biases in the
77 methodology did not reveal a mistake, however [47]. Furthermore, new experiments showed that
78 the problem nearly vanished when the angle between the radar beam and the perpendicular-to-*B*
79 direction was increased. Eventually, records were unearthed indicating that the temperature ratio
80 problem had always existed at Jicamarca but had been artificially “corrected” in the database [9]!
81 Indeed, the temptation to simply “correct” the problem in the modern era was strong too.

82 The temperature ratio problem ultimately pointed to a subtle problem with ISR theory at small
83 magnetic aspect angles arising from the neglect of electron Coulomb collisions [54, 55, 33, 44]. The
84 effect of Coulomb collisions on the ISR spectrum at small magnetic aspect angles is difficult to
85 capture and has not been formulated in closed form, and numerical estimates of the experimental
86 effects are expensive to calculate and store. There remains no completely satisfactory resolution to
87 the problem, although interim methods allow us to infer electron and ion temperatures from ISR
88 autocorrelation function measurements sufficiently well for most intents and purposes so long as
89 the magnetic aspect angle is not too small.

90 More importantly, the problem is now being investigated using a variety of avante garde methods
91 including large particle-in-cell (PIC) simulations, producing fundamental insights into transport
92 properties in kinetic plasmas and effective means of exploring them (see Longley et al. [40, 39]).
93 The research will very likely be more impactful in the end than the ionospheric energy balance
94 problem that motivated electron and ion temperature ratio measurements in the first place.

95 **2.2 Ionospheric irregularities**

96 Due to its frequency and its equatorial geometry, Jicamarca immediately encountered intense,
97 ubiquitous, and unexpected radar “clutter.” Fig. 1 shows a typical range-time-intensity plot
98 illustrating coherent backscatter observed at Jicamarca over a 24-hour period. The enhanced
99 backscatter comes from plasma density irregularities excited by different mechanisms including
100 neutral turbulence and plasma instabilities. Coherent scatter signifies free energy in the upper
101 atmosphere and is a distinctive telltale of space weather.

102 Incoherent scatter cannot be measured in regions of strong clutter which comes through the main
103 lobe and/or the sidelobes of all of Jicamarca’s antenna pointing positions. This prohibits a number
104 of desirable experiments from being performed. The scientific tradeoff of the clutter is favorable,
105 however, since coherent scatter offers keen insights into important processes in equatorial aeronomy
106 and space weather that might have gone unnoticed otherwise.

107 Near 100 km altitude, the equatorial electrojet, a strong current system confined to low magnetic
108 latitudes, flows. The current gives rise to both configuration-space and phase-space instabilities,
109 gradient drift and Farley Buneman instabilities respectively [53, 12]. The resulting plasma density
110 irregularities are strongly magnetic field aligned, as are irregularities in the *F* region and above.
111 The two instabilities are also closely coupled and described by a unified dispersion relation [16].

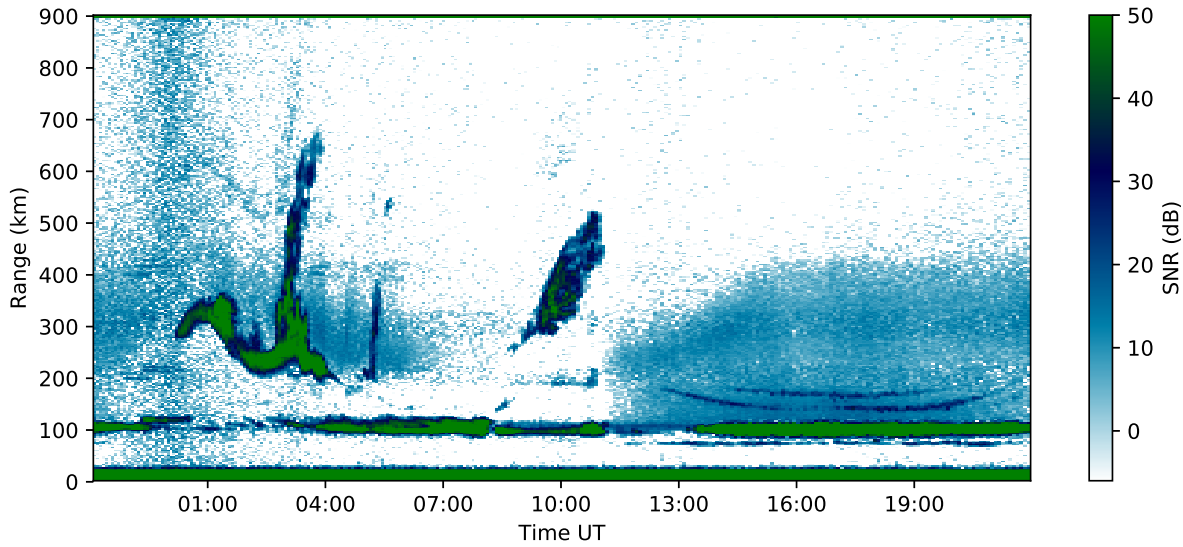


Figure 1. Range time intensity plot for Sep. 14, 2010, showing backscatter signal-to-noise ratio versus altitude and time. Note that UT = LT + 5 hr. Cyan hues mainly represent incoherent scatter whereas blue and green hues represent coherent scatter (see text).

112 The irregularities can be studied in detail near the magnetic equator where it is straightforward
 113 to distinguish echoes from different altitudes and where interferometry and imaging methods can
 114 be applied. Primary gradient drift waves can be observed at Jicamarca using interferometry and
 115 aperture-synthesis imaging, for example [31, 25]. Following their discovery at Jicamarca, similar
 116 instabilities were found to operate the auroral zone and, later, at middle latitudes. Farley Buneman
 117 instability has important implications outside equatorial aeronomy, altering the conductance of the
 118 auroral *E* region important for MI coupling [38] and causing heating in the solar chromosphere (e.g.
 119 [43]).

120 Below the electrojet irregularities are intermittent irregularities in the mesosphere. These
 121 represent fluctuations in the index of refraction driven by mesospheric turbulence and exaggerated
 122 by the presence of free electrons in the *D* region. While they are not unique to the equatorial zone,
 123 they can be readily observed at Jicamarca due to the 50 MHz frequency and the high sensitivity of
 124 the facility [58]. Neutral turbulence can be observed at Jicamarca in the mesosphere, stratosphere,
 125 and troposphere, and the discovery gave rise to the field of MST-radar techniques. Using these
 126 techniques, it is possible to measure neutral wind speeds, turbulence parameters, and turbulent
 127 fine structure [17, 52, 20, 34].

128 Above the electrojet and throughout the *F* region, ionospheric interchange instability driven by
 129 free energy in the postsunset bottomside *F* region density gradient produces deep deformations
 130 in the bottomside that can penetrate into the topside, producing towering plumes of coherent
 131 backscatter (see Fig. 1). The phenomenon underlies equatorial spread *F* (ESF) which is among the
 132 earliest space weather effects detected [3]. The association with interchange instability enjoyed
 133 considerable speculation but was not established until Woodman and La Hoz [59] produced
 134 definitive range-time-intensity (RTI) radar imagery of the process. (The authors reportedly needed

135 to justify the recent purchase of an expensive new Versatec printer and invented RTI-style figures
136 for this paper! The figures were very persuasive and remain the standard means of presentation.)

137 ESF remains the cause célèbre of equatorial aeronomy as it disrupts modern radio communication,
138 navigation, and imaging systems. Despite the fact that the underlying physics appears to be
139 well understood, accurate forecasts remain elusive [56]. Jicamarca contributes to the research
140 by measuring simultaneously both the causes (background ionospheric structure, vertical, and
141 east-west plasma drifts via ISR) and the effects (irregularity morphology via coherent scatter and
142 aperture synthesis imaging).

143 The interchange instabilities responsible for ESF are very similar to the $\mathbf{E} \times \mathbf{B}$ and current
144 convective instabilities that create irregularities in the auroral F region, i.e., the irregularities
145 monitored by the SuperDARN radar network. (The predecessor to SuperDARN, STARE, was an
146 effort to infer high-latitude convection patterns from auroral electrojet echoes on the basis of earlier
147 experiences from Jicamarca.) Some of the other irregularities in Fig. 1, meanwhile, are unique to
148 the equatorial zone. Their discoveries were contrary to orthodoxy and deserve special attention.

149 2.2.1 150-km echoes

150 Balsley [1] identified another persistent source of radar clutter in the daytime valley region between
151 about 140–170 km altitude in the early days of Jicamarca. Roervik and Miller [51], Roervik [50]
152 would associate the clutter with field-aligned plasma density irregularities, but it was not until a
153 decade later that mysterious “150-km echoes” would receive serious scientific attention. (Mysterious
154 because they exist in a homogeneous stratum of the ionosphere where gradient drift-type instability
155 should not occur.) Kudeki and Fawcett [32] investigated the layers with a new, high-resolution mode
156 and found them to be highly structured, exhibiting a stunning necklace shape that plunged with
157 decreasing solar zenith angle. Most remarkably, the Doppler shifts of the echoes seemed to match the
158 vertical plasma drifts. This suggested a means of measuring ionospheric dynamics using relatively
159 low power radar systems going forward. The correspondence between the 150-km echo Doppler
160 shifts at zenith with the vertical plasma drifts was established by Woodman and Villanueva [60].
161 Later, Chau and Woodman [8] would show that both the vertical and zonal plasma drifts could be
162 estimated accurately on the basis of line-of-sight 150-km echo Doppler shift measurements.

163 The source of the echoes remained a mystery for many more years. Two important clues helped
164 expedite the research. One was the discovery of two distinct types of echoes — one spectrally narrow
165 and field-aligned, and the other broad like a naturally enhanced ion line [6, 7]. The other was the
166 observation that the layer height and intensity reacted to solar flares [48] (see also [46]). The echoes
167 were clearly not due to some variant of gradient drift instability.

168 A pivotal finding came from Oppenheim and Dimant [45] who identified energetic photoelectrons
169 as the likely source of free energy behind the echoes. Their simulations reproduced narrow and
170 broad spectral features and predicted both enhanced ion and electron lines. The authors tentatively
171 associated their findings with upper hybrid instability [2, 29]. That association was made more
172 explicitly by Longley et al. [41] who pointed out that the gaps in the echo necklace structure
173 could be explained by cyclotron damping where the upper hybrid frequency matches an electron
174 gyroharmonic frequency. As shown by Lehmacher et al. [36], this implies that not only plasma drifts
175 but also plasma density profiles can be inferred from the 150-km echoes using low-power radar.

176 2.2.2 Bottom-type layers

177 Woodman and La Hoz [59] identified several types of coherent scatter echoes associated with
178 postsunset F -region instability. Among these were “bottom-type” or thin scattering layers that
179 serve as precursors for intense plume events. The layers do not have signatures in ionograms, total
180 electron content (TEC) measurements, radio scintillations, or airglow imagery and were neglected
181 by the aeronomy and space-weather communities. Since “ESF” is a term taken from ionospheric
182 sounding, if a phenomenon does not affect ionograms, it is not regarded as ESF. The bottom-type
183 layers were just another unfortunate source of clutter.

184 For decades after their discovery, it was taken for granted that bottom-type layers signified
185 marginal collisional interchange instability. There are several problems with this explanation,
186 however. First, the layers exhibit little or no vertical development over time whereas interchange
187 instabilities are convective instabilities and require vertical development. Second, the intensity of
188 the layers does not vary directly with the strength of the background zonal electric field as is
189 expected for the ionospheric interchange instability [61]. Thirdly, the layers form at the base of the
190 F region, near the valley, rather than in the steepest part of the bottomside where the growth rate
191 for interchange instability is greatest.

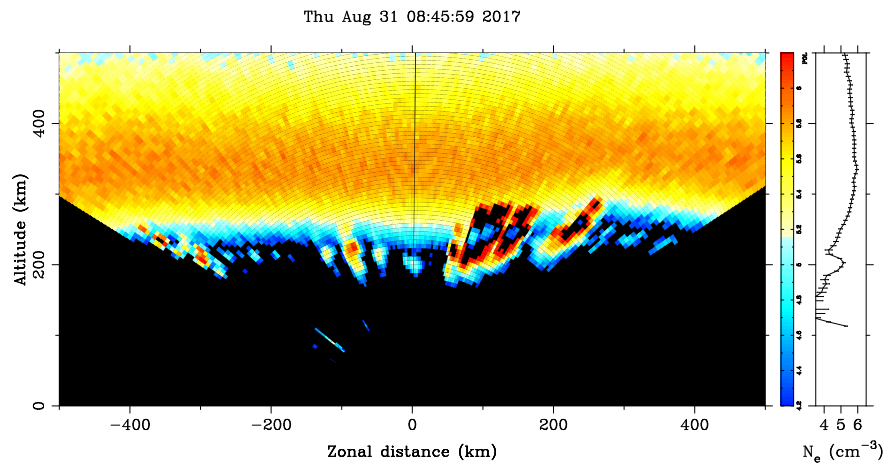


Figure 2. ALTAIR radar images showing bottom-type layers at the base of the F region just prior to the onset of ESF. The data were acquired during NASA project WINDY [28].

192 Three clues shed light on the significance of the layers. The first was that fine structure in
193 backscatter from the layers often exhibits horizontal striations [23]. This might be expected for
194 gradient drift-type instability driven by zonal winds near a horizontal density gradient. The second
195 was that the layers are not continuous but are patchy with horizontal scales of tens to hundreds of
196 km [27] (see Fig. 2). The third was that they exist at altitudes and times where the plasma flow is
197 westward – opposite the direction of the zonal neutral winds. Vertical shear flow predominates in
198 the postsunset bottomside ionosphere, and associated with the shear flow is strong vertical current
199 that is usually neglected in stability analysis [21].

200 Hysell and Kudeki [26] showed that the aforementioned vertical current destabilizes the ionosphere
201 to irregularities propagating at angles intermediate between the vertical and the horizon. The
202 instability has a larger growth rate than the ionospheric interchange instability but is confined to

203 a narrow stratum. The instability causes the bottomside to be corrugated and unstable to wind-
204 driven gradient drift instability in the ascending phases, explaining the bottom-type layers. Most
205 importantly, the irregularities precondition the ionosphere to interchange instability which can grow
206 more rapidly than it would otherwise. Numerical simulations show that this auxiliary instability is
207 required for ESF depletions and radar plumes to develop and penetrate the topside as quickly after
208 sunset as they do [24].

209 2.2.3 High-altitude echoes

210 In 2008, a problem was discovered with some of Jicamarca's routine ISR experiments. Noise
211 estimates were being calculated using samples from distant range gates above about 1,500 km. At
212 night, the noise estimates would sometimes become anomalously large. It appeared that the distant
213 range gates were being contaminated by signals of some kind. Further investigation showed that
214 intense scattering layers were present at very high altitudes, most often between midnight and
215 sunrise. At the time, a different method for estimating noise was introduced. The layers did not
216 receive special attention and eventually disappeared.

217 However, the high-altitude echoes returned during the next solar minimum, and this time they
218 were investigated further in a series of experiments beginning in 2018 and continuing to the present
219 [10]. It was found that, during low solar flux conditions, the echoes are common in the pre-dawn
220 sector between about 1,500–2,200 km altitude. The echoes exhibit Doppler shifts between about
221 ± 150 m/s and zonal drift rates of a few tens of m/s determined by multi-beam experiments. They
222 are not obviously related to ESF.

223 Most importantly, the echoes exhibit sidebands upshifted and downshifted from the carrier by
224 the lower hybrid frequency for protons. This is a remarkable result that is not well understood.
225 One candidate mechanism is lower hybrid drift instability [30, 18], a streaming instability similar
226 to modified two-stream instability, excited in this case by ion diamagnetic drift in the vicinity of
227 existing plasma density irregularities. Another candidate is linear mode conversion and/or resonance
228 instability in the vicinity of existing irregularities driven by lightning-induced whistlers [35]. The
229 former mechanism is related to one invoked to explain small-scale irregularities in ESF [22]. The
230 latter mechanism is similar to one invoked to explain explosive spread *F* [37]. In either case, pre-
231 existing irregularities are required to bootstrap the instability. The source of these could be ESF
232 although this is merely speculation at this point.

233 The high-altitude echoes represent frontier science in equatorial aeronomy with overtones for
234 adjacent research domains like lightning research and even magnetic reconnection. For many years,
235 however, they were just an overlooked source of radar clutter. In fact, the high-altitude echoes were
236 recognized in the early days of Jicamarca experiments but were neglected because of more pressing
237 problems making ISR experiments work.

3 CONCLUSIONS

238 This paper reviewed a number of discoveries in equatorial aeronomy and space physics going back
239 to the 1960s. In each case, the discoveries came from projects and experiments that did not go
240 according to plan. These were not merely serendipitous discoveries. Nor should they be considered
241 negative outcomes of hypothesis tests. Rather, in most cases, they were the byproducts of the
242 failures of assumptions that were not in doubt. Gyroresonances were supposed to be part of the

243 incoherent backscatter spectrum. Coulomb collisions were supposed to be negligible. ESF was
244 supposed to be driven entirely by ion interchange instability. The equatorial valley region and
245 the inner plasmasphere were supposed to be stable. Pursuing the problems furthermore required
246 deliberate departures from planned research. In some cases, this occurred only after long delays.

247 How can research be structured to make allowances for plans gone wrong and subsequent off-
248 plan excursions? The premise seems to be at odds with contemporary trends which favor decadal
249 planning for funding agencies, meticulous planning in research proposals, and long-range research
250 plans for applicants for even junior positions. Perhaps, as Eisenhower famously said, plans are
251 useless, but planning is indispensable. The important point is that it is essential to have the
252 freedom to pivot when plans fail and to pursue the discoveries which may lie beneath.

CONFLICT OF INTEREST STATEMENT

253 The author declares that the research was conducted in the absence of any commercial or financial
254 relationships that could be construed as a potential conflict of interest.

AUTHOR CONTRIBUTIONS

255 The Author performed all research on this perspective and wrote the manuscript.

FUNDING

256 This work was supported by award NNX15AL02G from the National Aeronautics and Space
257 Administration. The Jicamarca Radio Observatory is a facility of the Instituto Geofísico del Perú
258 operated with support from NSF award AGS-1732209 through Cornell. The help of the staff is
259 much appreciated.

ACKNOWLEDGMENTS

260 The author is indebted to Prof. Juha Vierinen who acquired and provided the data shown in Fig. 1
261 and to Prof. Jorge Chau for his helpful suggestions.

DATA AVAILABILITY STATEMENT

262 Data used for this publication are available through the Madrigal database (see <http://www.openmadrigal.org>).

REFERENCES

- 263 [1] Balsley, B. B. (1964). Evidence of a stratified echoing region at 150 kilometers in the vicinity
264 of magnetic equator during daylight hours. *J. Geophys. Res.* 69, 1925
- 265 [2] Basu, B., Chang, T., and Jasperse, J. R. (1982). Electrostatic plasma instabilities in the
266 daytime lower ionosphere. *Geophys. Res. Lett.* 9, 68–71
- 267 [3] Booker, H. G. and Wells, H. W. (1938). Scattering of radio waves by the *F* region. *Terres.*
268 *Magn.* 43, 249
- 269 [4] Bowles, K. L. (1963). Measuring plasma density of the magnetosphere. *Science* 139, 389–391,
270 <https://doi.org/10.1126/science.139.3553.389>

271 [5] Bowles, K. L., Ochs, G. R., and Green, J. L. (1962). On the absolute intensity of incoherent
272 scatter echoes from the ionosphere. *J. of Res. NBS - D. Rad. Prop.* 66D, 395

273 [6] Chau, J. L. (2004). Unexpected spectral characteristics of VHF radar signals from 150-km
274 region over Jicamarca. *Geophys. Res. Lett.* 31, L23803, doi:10.1029/2004GL021620

275 [7] Chau, J. L. and Kudeki, E. (2013). Discovery of two distinct types of equatorial 150-km radar
276 echoes. *Geophys. Res. Lett.* 40, 4509–4514, doi/10.1002/grl.50893

277 [8] Chau, J. L. and Woodman, R. F. (2004). Daytime vertical and zonal velocities from
278 150-km echoes: Their relevance to F-region dynamics. *Geophys. Res. Lett.* 31, L17801,
279 10.1029/2004GL020800

280 [9] Clark, W. L., McClure, J. P., and Van Zandt, T. E. (1976). *Description and Catalog of*
281 *Ionospheric F Region Data, Jicamarca Radio Observatory (November 1966 – April, 1969)*.
282 Tech. Rep. UAG-53, World Data Center A for Solar-Terrestrial Physics

283 [10] Derghazarian, S., Hysell, D. L., Kuyeng, K., and Milla, M. A. (2021). High altitude
284 echoes from the equatorial topside ionosphere during solar minimum. *J. Geophys. Res.* 126,
285 https://doi.org/10.1029/2020JA028424

286 [11] Dougherty, J. P. (1964). Model Fokker-Planck equation for a plasma and its solution. *Phys.*
287 *Fluids* 1, 1788

288 [12] Farley, D. T. (1963). A plasma instability resulting in field-aligned irregularities in the
289 ionosphere. *J. Geophys. Res.* 68, 6083

290 [13] Farley, D. T. (1964). The effect of Coulomb collisions on incoherent scattering of radio waves
291 by a plasma. *J. Geophys. Res.* 69, 197–200, 2402

292 [14] Farley, D. T. (1966). A theory of incoherent scattering of radio waves by a plasma, 4, The
293 effect of unequal ion and electron temperatures. *J. Geophys. Res.* 71, 4091–4098

294 [15] Farley, D. T. (1967). Proton gyroresonance observed in incoherent scattering from the
295 ionosphere. *Phys. Fluid.* 10, 1584–1586

296 [16] Fejer, B. G. and Kelley, M. C. (1980). Ionospheric irregularities. *Rev. Geophys.* 18, 401

297 [17] Fukao, S., Sato, T., Kato, S., Harper, R. M., Woodman, R. F., and Gordon, W. E. (1974).
298 Mesospheric winds and waves over Jicamarca on May 23–24, 1974. *J. Geophys. Res.* 84, 4379–
299 4386

300 [18] Gladd, N. T. (1975). The lower hybrid drift instability and the modified two stream instability
301 in high density theta pinch environments. *Plasma Physics* 18, 27–40

302 [19] Gordon, W. E. (1958). Incoherent scattering of radio waves by free electrons with applications
303 to space exploration by radar. *Proc. IRE* 46, 1824

304 [20] Guo, L., Lehmacher, G., Kudeki, E., Akgiray, A., Sheth, R., and Chau, J. L. (2007). Turbulent
305 kinetic energy dissipation rate and eddy diffusivity study in the tropical mesosphere using
306 Jicamarca radar data. *Adv. Space Res.* 40

307 [21] Haerendel, G., Eccles, J. V., and Cakir, S. (1992). Theory for modeling the equatorial evening
308 ionosphere and the origin of the shear in the horizontal plasma flow. *J. Geophys. Res.* 97, 1209

309 [22] Huba, J. D. and Ossakow, S. L. (1981). On 11-cm irregularities during equatorial spread F. *J.*
310 *Geophys. Res.* 86, 829

311 [23] Hysell, D. L. (1992). *On the hierarchy of processes contributing to equatorial spread F.* Ph.D.
312 thesis, Cornell Univ., Ithaca, N. Y.

313 [24] Hysell, D. L. (2022). Modeling equatorial F-region ionospheric instability using a regional
314 irregularity model and WAM-IPE. *J. Geophys. Res.*

315 [25] Hysell, D. L. and Chau, J. L. (2002). Imaging radar observations and nonlocal theory of
316 large-scale waves in the equatorial electrojet. *Ann. Geophys.* 20, 1167

317 [26] Hysell, D. L. and Kudeki, E. (2004). Collisional shear instability in the equatorial *F* region
318 ionosphere. *J. Geophys. Res.* 109, doi:10.1029/2004JA010636

319 [27] Hysell, D. L., Larsen, M. F., Swenson, C. M., Barjatya, A., Wheeler, T. F., Sarango, M. F.,
320 et al. (2005). Onset conditions for equatorial spread *F* determined during EQUIS II. *Geophys.*
321 *Res. Lett.* 32, L24104, doi:10.1029/2005GL024743

322 [28] Hysell, D. L., Rao, S., Groves, K. M., and Larsen, M. F. (2020). Radar investigation of
323 postsunset equatorial ionospheric stability over Kwajalein during project WINDY. *J. Geophys.*
324 *Res.* , <https://doi.org/10.1029/2020ja027997>

325 [29] Jasperse, J. R., Basu, B., Retterer, J. M., Decker, D. T., and Chang, T. (1995). High
326 frequency electrostatic plasma instabilities and turbulence layers in the lower ionosphere. In
327 *Space Plasmas: Coupling Between Small and Medium Scale Processes* (Geophysical Monograph
328 86, American Geophysical Union). 77–94

329 [30] Krall, N. A. and Liewer, P. C. (1971). Low-frequency instabilities in magnetic pulses. *Phys.*
330 *Rev. A* A, <https://doi.org/10.1103/PhysRevA.4.2094>

331 [31] Kudeki, E., Farley, D. T., and Fejer, B. G. (1982). Long wavelength irregularities in the
332 equatorial electrojet. *Geophys. Res. Lett.* 9, 684

333 [32] Kudeki, E. and Fawcett, C. D. (1993). High resolution observations of 150 km echoes at
334 Jicamarca. *Geophys. Res. Lett.* 20, 1987

335 [33] Kudeki, E. and Milla, M. (2011). Incoherent scatter spectral theories – part I: A general
336 framework and results for small magnetic aspect angles. *IEEE Trans. Geosci. Remote Sens.*
337 49(1), 315–328

338 [34] Lee, K., Kudeki, E., Reyes, P. M., Lehmacher, G., and Milla, M. (2019). Mesospheric wind
339 estimation with the Jicamarca MST radar. *Radio Sci.* 54, 10.1029/2019RS006892

340 [35] Lee, M. C. and Kuo, S. P. (1984). Production of lower hybrid waves and field-
341 aligned plasma density striations by whistlers. *J. Geophys. Res.* 89 (A12), 10,873–10,880,
342 doi:10.1029/JA089iA12p10873

343 [36] Lehmacher, G. A., Wu, H., Kudeki, E., Reyes, P. M., Hysell, D. L., and Milla, M. A.
344 (2020). Height variation gaps in 150-km echoes and Whole Atmosphere Community Climate
345 Model electron densities suggest link to upper hybrid resonance. *J. Geophys. Res.* 125,
346 <https://doi.org/10.1029/2019JA027204>

347 [37] Liao, C. P., Freidberg, J. P., and Lee, M. C. (1989). Explosive spread *F* caused by lightning-
348 induced electromagnetic effects. *J. Atmos. Terr. Phys.* 51, 751–758

349 [38] Liu, J., Wang, W. B., Oppenheim, M., Dimant, Y., Wiltberger, M., and Merkin, S. (2016).
350 Anomalous electron heating effects on the *E* region ionosphere in TIEGCM. *Geophys. Res.*
351 *Lett.* 43, 2351–2358, DOI:10.1002/2016GL068010

352 [39] Longley, W. J., Oppenheim, M. M., and Dimant, Y. S. (2019). Nonlinear effects of electron-
353 electron collisions on ISR temperature measurements. *J. Geophys. Res.* 123, 6313–6329,
354 <https://doi.org/10.1029/2019JA026753>

355 [40] Longley, W. J., Oppenheim, M. M., Fletcher, A. C., and Dimant, Y. S. (2018). ISR
356 spectra simulations with electron-ion Coulomb collisions. *J. Geophys. Res.* 123, 2990–3004,
357 <https://doi.org/10.1002/2017JA025015>

358 [41] Longley, W. J., Oppenheim, M. M., Pedatella, N. M., and Dimant, N. M. (2020). The
359 photoelectron-driven upper hybrid instability as the cause of 150-km echoes. *Geophys. Res.*
360 *Lett.* 47, <https://doi.org/10.1029/2020GL087391>

361 [42] Lorenz, E. N. (1963). Deterministic non-periodic flow. *J. Atmos. Sci.* 20, 130

362 [43] Madsen, C. A., Dimant, Y. S., Oppenheim, M. M., and Fontenla, J. M. (2013). The
363 multi-species Farley-Buneman instability in the solar chromosphere. *ApJ* 783, 10.1088/0004–
364 637X/783/2/128

365 [44] Milla, M. A. and Kudeki, E. (2011). Incoherent scatter spectral theories – part II: Modeling
366 the spectrom for modes propagating perpendicular to **b**. *IEEE Trans. Geosci. Remote Sens.*
367 49(1), 329–345

368 [45] Oppenheim, M. M. and Dimant, Y. S. (2016). Photoelectron-induced waves: A likely source
369 of 150 km radar echoes and enhanced electron modes. *Geophys. Res. Lett.* 43, 3637–3644,
370 doi:10.1002/2016GL068179

371 [46] Pedatella, N. M., Chau, J. L., Vierinen, J., Qian, L., Reyes, P., Kudeki, E., et al. (2019). Solar
372 flare effects on 150-km echoes observed over Jicamarca: WACCM-X simulations. *Geophys. Res.*
373 *Lett.* , 10,951–10,958, <https://doi.org/10.1029/2019GL084790>

374 [47] Pingree, J. E. (1990). *Incoherent scatter measurements and inferred energy fluxes in the*
375 *equatorial F-region ionosphere*. Ph.D. thesis, Cornell Univ., Ithaca, N. Y.

376 [48] Reyes, P. M. (2012). *Solar flare effects observed over Jicamarca during MST-ISR experiments*.
377 Master's thesis, University of Illinois at Urbana-Champaign

378 [49] Rodrigues, F. S., Nicolls, M. J., Woodman, R. F., Hysell, D. L., Chau, J. L., and Gonález,
379 S. A. (2007). Ion gyroresonance observations at Jicamarca revisited. *Geophys. Res. Lett.* 34,
380 <https://doi.org/10.1029/2007GL029680>

381 [50] Rojrvik, O. (1982). Drift and aspect sensitivity of scattering irregularities in the upper
382 equatorial E-region. *J. Geophys. Res.* 87, 8338

383 [51] Rojrvik, O. and Miller, K. L. (1981). Nonthermal scattering of radio waves near 150 km above
384 Jicamarca, Peru. *J. Geophys. Res.* 86, 180

385 [52] Sheth, R., Kudeki, E., Lehmacher, G. E., Sarango, M., Woodman, R., Chau, J. L., et al.
386 (2006). A high-resolution study of mesospheric fine structure with the Jicamarca MST radar.
387 *Ann. Geophys.* 24, 1281–1293

388 [53] Simon, A. (1963). Instability of a partially ionized plasma in crossed electric and magnetic
389 fields. *Phys. Fluids* 6, 382

390 [54] Sulzer, M. P. and Gonzalez, S. (1999). The effect of electron Coulomb collisions on the
391 incoherent scatter spectrum in the F region at Jicamarca. *J. Geophys. Res.* 104, 22,535–22,552

392 [55] Woodman, R. F. (2004). On a proper electron collision frequency for a Fokker-Planck collision
393 model with Jicamarca applications. *J. Atmos. Sol. Terr. Phys.* 66.17, 1521–1541

394 [56] Woodman, R. F. (2009). Spread F- An old equatorial aeronomy problem finally resolved? *Ann.*
395 *Geophys.* 27, 1915–1934

396 [57] Woodman, R. F., Farley, D. T., Balsley, B. B., and Milla, M. A. (2019). The early history of
397 the Jicamarca Radio Observatory and the incoherent scatter technique. *Hist Geo Space. Sci.*

398 [58] Woodman, R. F. and Guillén, A. (1974). Radar observations of winds and turbulence in the
399 stratosphere and mesosphere. *J. Atmos. Sci.* 31, 493–505

400 [59] Woodman, R. F. and La Hoz, C. (1976). Radar observations of F region equatorial irregularities.
401 *J. Geophys. Res.* 81, 5447–5466

402 [60] [Dataset] Woodman, R. F. and Villanueva, F. (1995). Comparison of electric fields measured
403 at F region heights with 150 km irregularity drift measurements. Proceedings of the Ninth
404 International Symposium on Equatorial Aeronomy. Bali, Indonesia, March 20-24
405 [61] Zargham, S. and Seyler, C. E. (1987). Collisional interchange instability, 1, Numerical
406 simulations of intermediate-scale irregularities. *J. Geophys. Res.* 92, 10,073